INDIAN INSTITUTE OF TECHNLOGY, KANPUR

GPS denied Localization and Magnetometer-Free Yaw Estimation for UAVs

Author:
Naveen Balaji
Undergraduate Student

Supervisor:
Dr. Mangal Kothari
Associate Professor

End-Term Report for the project done in the

Intelligent Guidance and Control Laboratory
Aerospace Department
IIT Kanpur

November 18, 2019

Abstract

This paper presents a range-based localization scheme for multi-rotor systems in GPS denied environments and proposes a novel methodology to estimate yaw attitude. The attitude and position are estimated using a Bayesian framework using accelerometers, gyroscope, and a set of ultra-wideband (UWB) range sensors, with an optimization technique for tuning of the estimator's parameter (covariance matrices). In addition to this, heading estimation is incorporated without the aid of magnetic sensors. Extended Information Filter (EIF), which is dual of Kalman filter, is used to reduce time complexity in the localization. All family of Gaussian filters requires the correct noise parameters for convergence and efficient estimation. A Particle-Swarm Optimization (PSO) method is used for the tuning of noise covariance in these filters with known ground truth in the initial flight. The effectiveness of tuned EIF is validated on the quadcopter platform with different environments which shows superior performance compared to the manually picked noise parameter.

Keywords:- Unmanned Aerial Vehicles, Gaussian filters, Swarm Robotics, GPS denied Navigation

.

Contents

Chapter 1

Introduction

Autonomous aerial systems capable of sensing and perceiving the environment have been the area of intense research due to their limitless applications, ranging from surveillance, precision agriculture, infrastructure inspection, photography, recreation etc. Unmanned Aerial Systems (UAS), such as quadcopters and unmanned helicopters, offer robust maneuverability with vertical takeoff and hovering capabilities on the three-dimensional airspace. They can perform tracking [13], inspections [19], and transportation [21] more quickly, economically, and safely compared to other comparable robots. The deployment of sophisticated sensors is incrementally enhancing the intelligence of these aerial robots [8], enabling them to achieve autonomous navigation in complex and confined environments. The applications related to inspection and surveillance of commercial installations require these UAS to operate in GPS shadow areas where GPS signal reception may be diminished and less reliable. Further, the reliance of magnetometer for heading estimate is severely compromised if the UAS has to operate near large iron structures such as large cranes due to magnetic deviation.

Indoor Positioning System (IPS) becomes critical for many autonomous operations requiring application of UAS in GPS denied environments. Visual odometry for mobile robotics using feature tracking based on monocular and stereo-vision has been an active area of research to address indoor localization [23, 3, 4]. However, the solutions are sensitive to ambient lighting conditions, motion blur, and other artifacts that deteriorate image quality. Visual-inertial methods improved localization precision by eliminating scale factor error in the image with the fusion of inertial measurement unit (IMU) data [9]. The accumulation of drift in these methods are typical over time, thus cannot be used for long duration flights. Other SLAM based approaches popular among ground robots either use RGB-D cameras [12] or 3D lidars [25]. However, these approaches are often computationally expensive and time-intensive. They typically require onboard GPU computing ability to process the data in real-time, which increases the power requirements and the overall weight of the system, thereby further compromising the endurance of aerial vehicle.

The wireless localization system, such as Radio Frequency Identification (RFID) [27], Wi-Fi [20], Zigbee [24] and Ultra-Wideband (UWB) [5], are emerging technologies for indoor localization solutions. Due to the unsatisfied accuracy of the received signal strength (RSS) techniques [22], they have not been found suitable for UAVs. Recently, UWB based technologies have gained momentum in this field. With the large bandwidth, this signal has the properties of strong multi-path resistance, which enables accurate ranging via communication by the two-way time of flight. They are low-cost, low-power, portable, robust and easy to implement in any environment.

The present work is an extension of the approach followed in [11], which focused on developing a pose estimation framework for a quadcopter relying on MARG (inertial) sensor array, an optical flow camera, and an Ultra-wideband (UWB) range sensor to correct the drift of the estimator over time. In this paper, use of multiple UWB sensors is proposed along with inertial sensors without any optical cameras for localization. Although some earlier research has focused on implementing Bayesian filter based state estimation using UWB sensors [18, 15], it did not focus on optimizing the performance. The method used in this research aims to reduce the complexity of the algorithm using the extended information filter. The Gaussian filters require a model of the system, comprising of a state function, measurement function, and the associated noise terms. The noise terms related to it are often difficult to estimate. The inaccurate noise model can cause perturbation in the estimation, which will lead to divergence of the filter. There are optimal ways to adapt a filter according to the need [26]. Noise covariance can be estimated by minimizing the cost function, with the known ground truth of the vehicle. In this paper, various criteria for tuning the filter are discussed, and the Particle Swarm Optimization (PSO) is used for determining the best noise covariance.

Real-time tracking of the heading angle in rigid bodies has wide applications in robotics fields [6]. Inertial and magnetic sensor modules with their associated data filtering algorithms are designed for estimating the attitude of the object [17]. The famous estimation algorithms such as [16], allows accurate evaluation of pitch and roll attitude but are not robust for yaw estimations over time. The sources of magnetic interference are always present in common items such as current-conducting wires, batteries, and ferrous materials. Today there are many hybrid solutions such as [7], with expensive multiple sensors, to be used in the industrial environment for the estimation of the heading. This paper proposes to solve the problem of yaw estimation through a novel low-cost yaw estimation method without drift which can be used on UAS as fail-safe in the event of deterioration in yaw estimates from conventional MEMS magnetometers.

The remainder of the paper is structured as follows: the background work and problem statement is summarized in Sec. II. The localization and heading algorithms are given in Sec. III. The method of tuning the noise parameters based on PSI is given in Sec.IV. The experimental results and discussion are provided in Sec. V and concluding remarks are given in Sec. VI.

Chapter 2

BACKGROUND

2.1 Ultra-Wide Band Sensors

UWB sensor is a wireless sensor that transmit signals at 3-8 (GHz) bandwidth, offers high accuracy of signal with low power. It can measure distance through Time of Flight (ToF) of the radio signal, providing measurement range up to 200 m. The commercial-off-the-shelf UWB product Decawave DWM1001 [1] modules are used for the implementation of methodology proposed in the current paper. DWM1001 module has two modes: anchor mode (sending signal) and tag mode (receiving signal). The modules provides real-time location by the two-way ranging method. Then repeated reply algorithm is used to measure the time of flight between a tag and an anchor module. By subtracting the locally measured processing time $(Q^{Rx}_{M_2} - Q^{Rx}_{M_1})$ from the round-trip time $(Q^{Rx}_{M_1} - Q^{Tx}_{M_0})$ of the signal, the time of flight (TOF) can be estimated by

$$Z_{ToF} = Q^{Rx}_{M_1} - Q^{Tx}_{M_0} - \delta_Q \tag{2.1}$$

The detail explanation of range estimation using two-way ranging method is available in [10].

2.2 Problem Statment

The primary aim of this work is to localize an aerial vehicle (quadcopter) using IMU and UWB sensors. The UWB sensors are arranged at the corners of a rectangle to maintain a line-of-sight to the quadcopter as shown in Fig. 2.1. The current work uses a 3-axis MEMS accelerometer, a 3-axis MEMS gyroscope, and a 3-axis MEMS magnetometer as the inertial sensors equipped in the flight controller, which is a low-cost Invensense MPU6000 series. For magnetometer-free yaw estimation, measurements from magnetometer are discarded and another set of position measurement is used using another UWB sensor, the details are given in the next section. Bias in both acceleration and angular velocity is considered and explicitly estimated. All these sensors provide information on their local body frame. Due to the inconsistency of built-in barometer in the flight controller, a one-dimensional lidar in also incorporated to measure the altitude of the vehicle accurately. The ground truth reference is obtained using an eight camera Vicon motion capture system in indoor that provides precise estimates at 100 Hz.

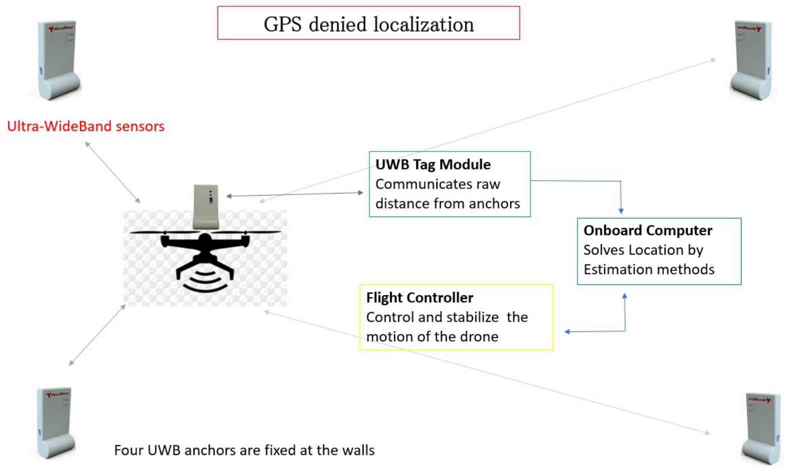

FIGURE 2.1: The UWB sensors based localization architecture

For control, the multi-copter position controller in PixHawk is initially tuned with the motion capture system. A Raspberry Pi 3 running Ubuntu mate is used as an onboard computer. Robot Operating System (ROS) environment is used for the state estimator implementation that communicates with the flight controller to provide high-level position and heading commands via the mavlink protocol. The quadcopters generally provide their local orientations, acceleration with respect to ENU (East-North-Up) frame. Since the UWB anchors used in current study are set up in a different direction, the UWB position estimates need to be transformed to ENU frame by rotating with the yaw offset before sending this data to the flight controller.

Chapter 3

Localization

In this section, a localization problem using UWB sensors in a given environment is considered. The suite of UWB sensors acts as GPS and is integrated with IMU to provide accurate localization. Let A, B, C, D be the position of fixed anchors, as shown in Fig. 3.1, with respect to the inertial frame of reference. Let $p = (px, py, pz)$ be the vehicle co-ordinate that need to be estimated by a localization algorithm when provide with distances $d1$, $d2$, $d3$, and $d4$ as follows:

$$(P - A)^2 = d_1^2; \quad (P - B)^2 = d_2^2; \quad (P - C)^2 = d_3^2; \quad (P - D)^2 = d_4^2;$$

The above set of equations can be solved either using nonlinear least square (NLS) method or using a (Bayesian) filter. As known the solution of NLS is corrupted with noise, therefore the filter based method is employed in this work. Extended Information Filter (EIF) is used due to its ease of implementation and time complexity.

3.1 Extended Information Filter

The EIF is an algebraic equivalent of the EKF in which Gaussian is parametrized by information vector, ξ, and information matrix, Ω, rather than the mean and covariance. For nonlinear state estimation with multi-sensor measurements, the EIF is preferred over the EKF. The prediction and update steps of EIF for localization are described below:

Prediction Step

The inertial sensor, accelerometer and gyroscope data is used for prediction. A constant acceleration model is considered for prediction step with acceleration bias, $a_b = [a_{bx},\ a_{by},\ a_{bz}]$. The state transition model is given as

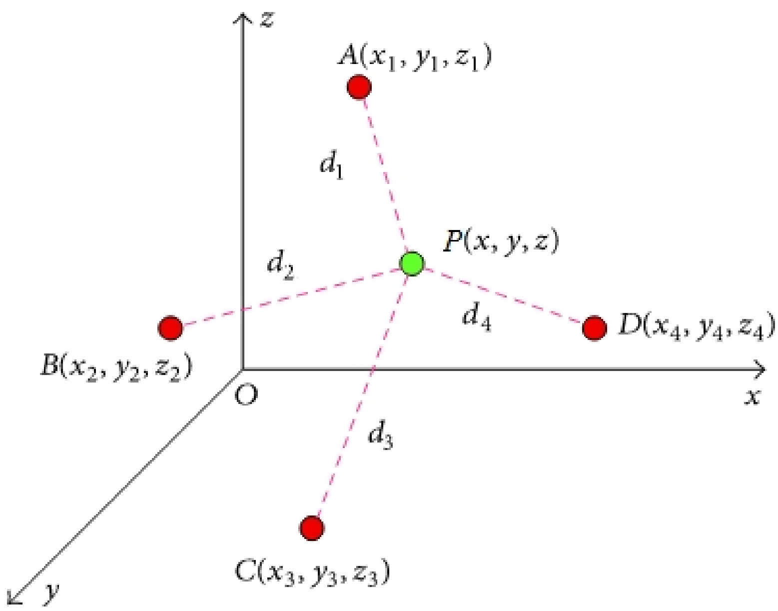

FIGURE 3.1: Point form of the problem statement

follows:

$$p_k = p_{k-1} + v_k\,T + \frac{a_k\,T^2}{2} - \frac{a_{bk}\,T^2}{2} \tag{3.1}$$

where p is the position vector, v is the velocity, the acceleration vector given by

$$a_k = R_k\,\vec{a}_{kbody} + \vec{g}$$

at k^{th} time step, and T is time interval taken for integration. Here R is a rotation matrix from the body to inertial frames. The state vector for localization and bias estimation is defined as

$$x = [p_x\,, v_x,\, a_{bx}\,, p_y\,, v_y\,, a_{by}\,, p_z\,, v_z\,, a_{bz}\,]^T$$

Having defined this, the information vector and matrix are given as follows:

$$\xi_k = \Sigma_k^{-1}\,x_k \qquad\qquad \Omega_k = \Sigma_k^{-1} \tag{3.2}$$

where Σ_k is the covariance matrix at time step k. The prediction steps are given as

$$\hat{\xi}_k = \hat{\Omega}_k \left(A_k\,\Omega_{k-1}^{-1}\,A_k^T + B_k\,u_k\right) \tag{3.3}$$

$$\hat{\Omega}_k = \left(A_k\,\Omega_{k-1}^{-1}\,A_k^T + Q_k\right)^{-1} \tag{3.4}$$

where $u_k = [\, a_{xK},\ 0,\ 0,\ a_{yK},\ 0,\ 0,\ a_{zK},\ 0,\ 0\,]^T$ and

$$A_k = \begin{bmatrix} A_k^{'} & 0 & 0 \\ 0 & A_k^{'} & 0 \\ 0 & 0 & A_k^{'} \end{bmatrix},\ A_k^{'} = \begin{bmatrix} 1 & T & \frac{-T^2}{2} \\ 0 & 1 & -T \\ 0 & 0 & 1 \end{bmatrix}$$

$$B_k = \begin{bmatrix} B_k^{'} & 0 & 0 \\ 0 & B_k^{'} & 0 \\ 0 & 0 & B_k^{'} \end{bmatrix},\ B_k^{'} = \begin{bmatrix} \frac{-T^2}{2} & 0 & 0 \\ T & 0 & 0 \\ 0 & 0 & 0 \end{bmatrix}$$

where Q_k is the process noise. The process noise matrix is ideally modeled, in order to obtain the Markov property, which is required in recursive Bayesian inference. It is assumed that Q_k is a function of a single variable (τ_a for a_{world} and τ_b for a_{bias}) which is approximated to be constant over time [14]. The continuous time zero-mean white noise modeled with bias superposition for the system is:

$$Q_k^{'} = \begin{bmatrix} \frac{T^3\tau_a}{3} + \frac{T^5\tau_b}{20} & \frac{T^2\tau_a}{2} + \frac{T^4\tau_b}{8} & -\frac{T^3\tau_b}{6} \\ \frac{T^2\tau_a}{2} + \frac{T^4\tau_b}{8} & T^2\tau_a + \frac{T^3\tau_b}{3} & -\frac{T^2\tau_b}{2} \\ -\frac{T^3\tau_b}{6} & -\frac{T^2\tau_b}{2} & -T^3\tau_b \end{bmatrix}$$

UWB Measurement Update

The range measurements obtained from the UWB senors for the update equation is

$$r_k = \left[\sqrt{(px - px_i)^2 + (py - py_i)^2 + (pz - pz_i)^2} \right]$$

where (px_i, py_i, pz_i) is the known position of anchor modules. The measurement update is carried out as following

$$\xi_k = \hat{\xi}_k + H_k^T R_k^{-1}[r_k - h(\hat{x}_k) + H_k\, \hat{x}_k] \tag{3.5}$$

$$\Omega_k = \hat{\Omega}_k + H_k^T R_k^{-1} H_k \tag{3.6}$$

where h_k is the measurement model given by r_k, $h(\hat{x}_k)$ is computed at $\hat{x}_k$,

$$H_k = \frac{\partial h}{\partial x_k} = \left[\frac{px - px_i}{\bar{r}_k}, 0, 0, \frac{px - px_i}{\bar{r}_k}, 0, 0, \frac{px - px_i}{\bar{r}_k} \right]^T$$

. In the above equation, R_k is measurement noise. In addition to this, the median filter ise used to remove the outliers of UWB readings that will result in a sudden change of the estimated position. The difference between the predicted distance $h(\hat{x}_k)$ and the actual UWB measurements r_k as $d_k = |h(\hat{x}_k) - r_k|$ is calculated and if the error term is over a certain threshold, the measurement is discarded.

Height Measurement Update

The altitude measurement obtained from the 1D lidar for update step is

$$l_k = [z]$$

The measurement matrix for updating height $[z]$ is

$$H_k = [\,0,\, 0,\, 0,\, 0,\, 0,\, 0,\, 1,\, 0,\, 0\,]$$

The information vector and matrices are updated using (3.5) and (3.6).

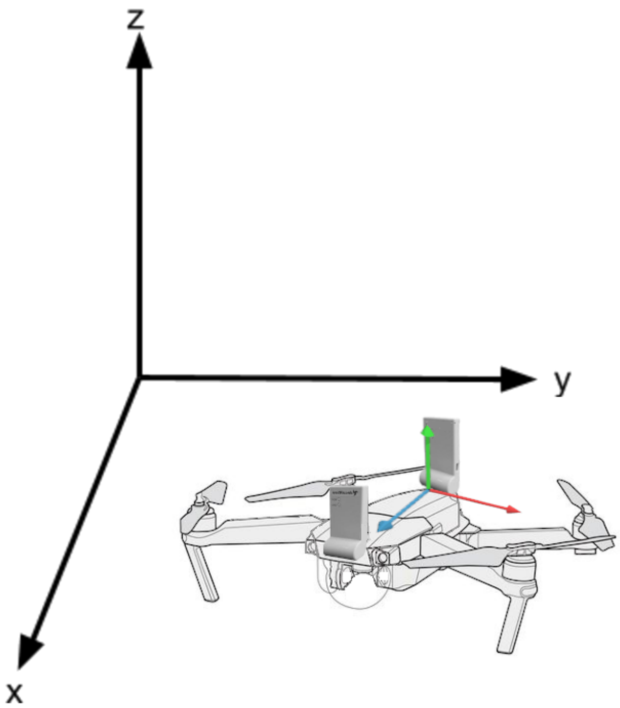

FIGURE 3.2: Yaw Estimation in fixed inertial frame

3.2 Yaw Estimation

For the yaw estimation, the UAS system is enhanced by mounting two UWB sensors on the quadcopter along with MARG sensors, as shown in Fig. 3.2. In order to determine yaw, the position of each sensor is estimated first using the approach described above. The modified state vector is given as

$$\mathbf{x} = [p_{x1}\,, p_{x2}\,, v_x\,, a_{bx}\,, p_{y1}\,, p_{y2}\,, v_y\,, a_{by}\,, p_{z1}\,, p_{z2}\,, v_z\,, a_{bz}\,, \theta\,]^T$$

Using these position, the yaw measurement is computed as

$$\theta = \cos^{-1}\left(\frac{p_{x2} - p_{x1}}{d_k}\right)$$

where

$$d_k = \sqrt{(p_{x2} - p_{x1})^2 + (p_{y2} - p_{y1})^2 + (p_{z2} - p_{z1})^2}$$

. The control vector, u, now has a extra input, ω, about the fixed inertial frame z-axis. For The dynamics is the same as described in the previous section. The Jacobin computed for this correction step is the

$$H_k = [\ \frac{\sqrt{{d_k}^2 - (p_{x2} - p_{x1})^2}}{{d_k}^2}, -\frac{\sqrt{{d_k}^2 - (p_{x2} - p_{x1})^2}}{{d_k}^2}, 0, 0,$$

$$-\frac{(p_{y2} - p_{y1}).(p_{x2} - p_{x1})}{{d_k}^2.\sqrt{{d_k}^2 - (p_{x2} - p_{x1})^2}}, \frac{(p_{y2} - p_{y1}).(p_{x2} - p_{x1})}{{d_k}^2.\sqrt{{d_k}^2 - (p_{x2} - p_{x1})^2}}, 0, 0,$$

$$-\frac{(p_{z2} - p_{z1}).(p_{x2} - p_{x1})}{{d_k}^2.\sqrt{{d_k}^2 - (p_{z2} - p_{x1})^2}}, \frac{(p_{z2} - p_{1}).(p_{x2} - p_{x1})}{{d_k}^2.\sqrt{{d_k}^2 - (p_{x2} - p_{x1})^2}}, 0, 0, 1\ ]^T$$

The roll and pitch attitude are estimated by the internal attitude heading reference system (AHRS) using IMU, which provide reasonable estimates in different operating conditions. In our experiment, the state estimation is carried out at 30Hz. Other sensors output frequency are lidar (20HZ), 2 [4 UWB sensors (10HZ)].

Chapter 4

Tuning

4.1 Learning the filter parameters

The learning techniques used for obtaining the noise parameters of EIF described in the previous section is described in this section. For simplicity, the discussion focuses on learning state-model and sensor noises, assuming that the dynamics considerations in vehicle state-model equations are perfect. Thrun and Andrew [2] have discussed various methods to train the noise parameter for the Kalman filter during the initial test. In this work, the minimization of residual prediction error is considered. The prediction error minimization technique seeks the parameter R and Q (assumed to be constant) that minimizes the quadratic deviation of z (ground truth) and its expectation, weighted by information matrix Ω.

$$< Q_{res}, R_{res} > = arg \min_{R,Q} \sum_{t=0}^{N} (z_t - \nu_t)\Omega_t(z_t - \nu_t)^T \tag{4.1}$$

where N is the total number of steps considered for training.

4.1.1 PSO implementation

The PSO was derived from the concept of swarming habits of animals such as birds or fish and have been implemented for many applications. The PSO algorithm maintains multiple potential solutions at one time and consists these steps: (i) Evaluate the fitness of each particle; (ii) Update individual and global bests; and (iii) Update velocity and position of each particle. In the tuning process, the filter covariance matrices, Q and R, are estimated as follows. At first, the noise matrices are reduced as a function of a single variable for simplicity. The problem is posed as to find best fit system noise (τ_a), inertial system bias noise (τ_b), and noise of UWB (R) subject to (4.1). The pseudo code of implementation is given in Algorithm 1. The weights c1, c2, c3 constraints the searching time and space. The number of iteration and particles should be chosen based on the desired accuracy.

Algorithm 1 PSO implementation

CostFunction (particle_i)

```
(τ_a, τ_b, R) = particle_i.pose
Evaluate(τ_a, τ_b, R) {residual prediction error}
returns error
```

Update_velocity (particle_i)

```
vel_cognitive = c1 (pose_best_i − self.position_i)
vel_social = c2 (global_best_pose − self.position_i)
Total_velocity= c3.velocity_i+vel_cognitive+vel_social
returns velocity
```

```
number of particles =10
Initialize all 10 particles with suspected (τ_a, τ_b, R)
max_iteration = 30
for i in max_iteration do
    for j in number of particles do
        Costfunction(particle_j)
        if particle_j.error < particle_j_min_error then
            particle_j_pose_best = particle_j.pose
            particle_j_minerror = particle_j.error
        end if
        if particle_j.error < global_min_error then
            particle_j.pose_best = global_best_pose
            particle_j.minerror = global_min_error
        end if
        for j in number of particles do
            Update_velocity(particle_j)
            particle_j.pose=particle_j.pose+particle_j.velocity
        end for
    end for
end for
return(global_best_pose)
```

Chapter 5

Results

5.1 Experimentation results

A series of experiments in the indoor lab setup are performed to demonstrate the accuracy of our position and attitude estimator on a quadcopter model. We first analyze the result of hand-tuned EIF covariance based on the property of system and measurement noises. Then, the training data set for establishing the ground truth is collected using motion capture system. The tuning of covariance is performed offline using the optimization method described in the previous section. The next set of experiments is conducted with the optimized noise parameters.

Position Estimation Accuracy

The initial experiment is conducted using a single UWB receiver (tag) placed on the quadcopter for simple position estimation. The initialization of position in EIF is done by least square method. There is no drift in the system; the quadcopter is able to maintain position hold for long duration. The UWB range sensor is accurately localized within error range of 0.2m when compared to ground truth values. The use of sonar in indoor gave good results in the z height estimates as compared inbuilt barometer data. The z RMS error for the localization comes out to be 0.048m.

Attitude accuracy

The roll and pitch attitude estimation is given by regular algorithm on Pixhawk stack. The heading angle estimated by this method suffered constant deflection in the indoor environment. Two UWB's are placed on quadrotor for yaw estimation. Our solution for yaw estimation has no deflections and no drift over time. The gyroscope (ω) about vertical axis is able respond to

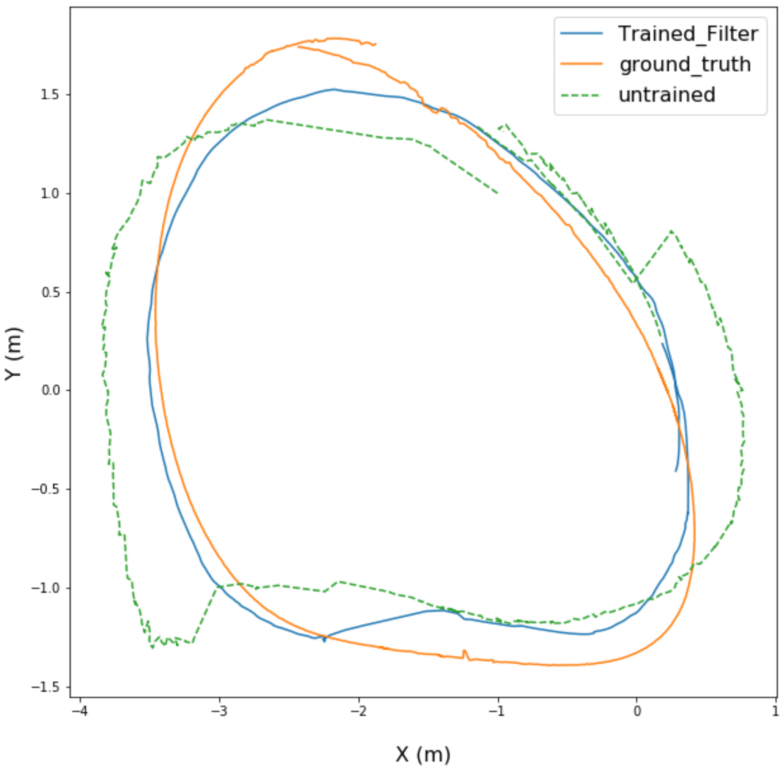

(A) Trajectory of state estimator in x-y plane

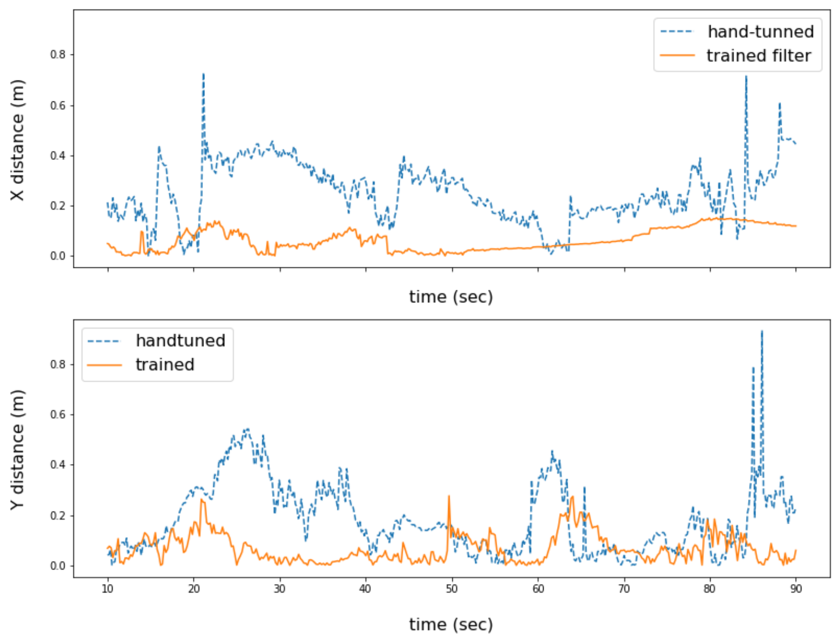

(B) Position error in x and y directions

FIGURE 5.1: Indoor Localization Results of the quadcopter

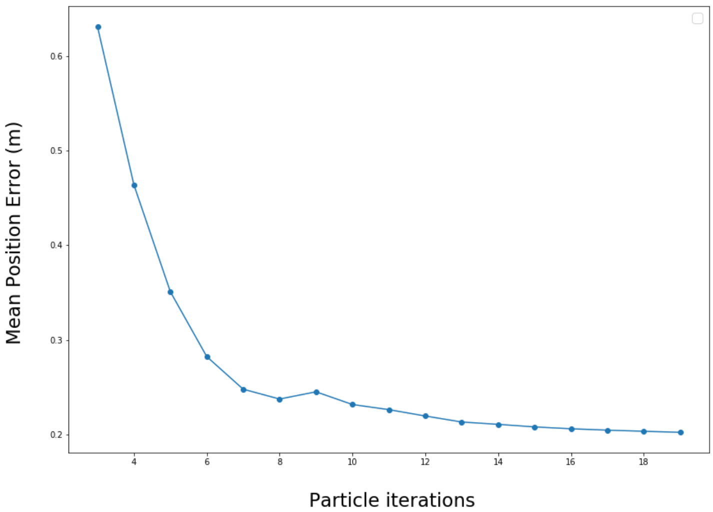

FIGURE 5.2: Convergence of cost function error in PSO algorithm

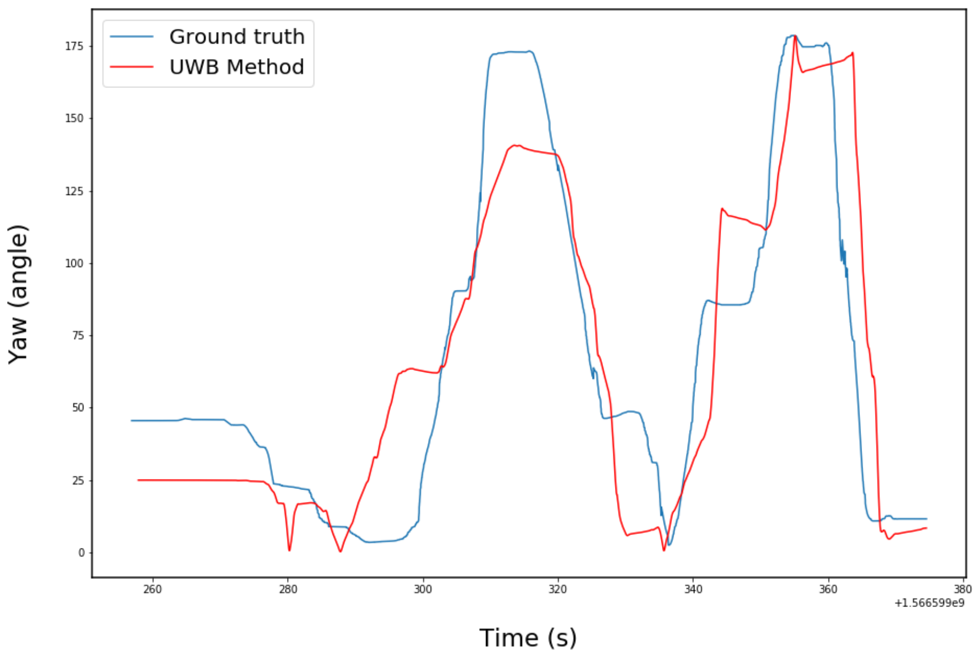

FIGURE 5.3: Accuracy of yaw estimation

the precise change in angle at 100Hz; the UWB sensors are able to keep the system from drifting away, unlike the magnetic compass.

Training accuracy

The hand-tuned filter noises fit well in some instances but when the aggressive maneuvers are performed, the filter sensitivity is inadequate. The optimization method of determining covariance with the training data is a quick process and results in precise results. The PSO algorithm valuated with weight $c1 = 1$, $c2 = 1$, $c3 = 0.55$ converged within 30 iterations and provided us $\tau_a = 0.151$, $\tau_b = 1.37$ and $R = 0.18$. The latency is tested by conveying this pose back to the flight controller, for predefined trajectory navigation. The quadcopter is able to perform well in offboard mode using this localization process.

Position Error	X axis	Y axis	Z axis	YAW
Untrained EIF	0.273m	0.257m	0.063m	0.28 (rad)
Trained EIF	0.166m	0.189m	0.048m	0.17 (rad)

TABLE 5.1: Performance of Localization

Chapter 6

Conclusion

In this paper, We discussed a novel localization methodology that can be used on aerial vehicles for industrial automation, irrespective of the environmental conditions, and external interference. The position and yaw estimation were implemented based on Information filter; the results are observed to be driftless over time. Next, the tuning of the filter parameters is performed using PSO. The optimization technique is used to obtain noise covariance based on minimum prediction criteria. Experiments conducted both in the indoor and outdoor environment validated the fitness of the approach. We conclude from the performance of this approach in the flight test that it can be deployable for the realistic environment. The yaw estimates obtained are promising and can be used as a failsafe to revert to in case of large magnetic deviation in conventional MEMS magnetometer. The proposed solution can be extended to coordinate multiple vehicles in the indoor arena in real-time.

Bibliography

[1] Decawave dwm1001 datasheet. https://www.decawave.com/. (Accessed on 10/09/2019).

[2] Pieter Abbeel, Adam Coates, Michael Montemerlo, Andrew Y Ng, and Sebastian Thrun. Discriminative training of kalman filters. In *Robotics: Science and systems*, volume 2, page 1, 2005.

[3] Markus Achtelik, Michael Achtelik, Stephan Weiss, and Roland Siegwart. Onboard imu and monocular vision based control for mavs in unknown in-and outdoor environments. In *2011 IEEE International Conference on Robotics and Automation*, pages 3056–3063. IEEE, 2011.

[4] Markus Achtelik, Abraham Bachrach, Ruijie He, Samuel Prentice, and Nicholas Roy. Stereo vision and laser odometry for autonomous helicopters in gps-denied indoor environments. In *Unmanned Systems Technology XI*, volume 7332, page 733219. International Society for Optics and Photonics, 2009.

[5] Abdulrahman Alarifi, AbdulMalik Al-Salman, Mansour Alsaleh, Ahmad Alnafessah, Suheer Al-Hadhrami, Mai Al-Ammar, and Hend Al-Khalifa. Ultra wideband indoor positioning technologies: Analysis and recent advances. *Sensors*, 16(5):707, 2016.

[6] Billur Barshan and Hugh F Durrant-Whyte. Inertial navigation systems for mobile robots. *IEEE Transactions on Robotics and Automation*, 11(3):328–342, 1995.

[7] Michael Bentley. Wireless and visual hybrid motion capture system, April 26 2016. US Patent 9,320,957.

[8] Guowei Cai, Jorge Dias, and Lakmal Seneviratne. A survey of small-scale unmanned aerial vehicles: Recent advances and future development trends. *Unmanned Systems*, 2(02):175–199, 2014.

[9] Jeffrey Delmerico and Davide Scaramuzza. A benchmark comparison of monocular visual-inertial odometry algorithms for flying robots. In *2018*

IEEE International Conference on Robotics and Automation (ICRA), pages 2502–2509. IEEE, 2018.

[10] Igor Dotlic, Andrew Connell, Hang Ma, Jeff Clancy, and Michael McLaughlin. Angle of arrival estimation using decawave dw1000 integrated circuits. In *2017 14th Workshop on Positioning, Navigation and Communications (WPNC)*, pages 1–6. IEEE, 2017.

[11] Krishnraj S Gaur, Hardik Parwana, Ajay Bhatt, Gaurav Pandey, and Mangal Kothari. Low cost solution for pose estimation of quadrotor. In *2018 AIAA Information Systems-AIAA Infotech@ Aerospace*, page 0466. 2018.

[12] Christian Kerl, Jürgen Sturm, and Daniel Cremers. Dense visual slam for rgb-d cameras. In *2013 IEEE/RSJ International Conference on Intelligent Robots and Systems*, pages 2100–2106. IEEE, 2013.

[13] Jongrae Kim and Yoonsoo Kim. Moving ground target tracking in dense obstacle areas using uavs. *IFAC Proceedings Volumes*, 41(2):8552–8557, 2008.

[14] Roger Labbe. Kalman and bayesian filters in python. 2015.

[15] Jiaxin Li, Yingcai Bi, Kun Li, Kangli Wang, Feng Lin, and Ben M Chen. Accurate 3d localization for mav swarms by uwb and imu fusion. In *2018 IEEE 14th International Conference on Control and Automation (ICCA)*, pages 100–105. IEEE, 2018.

[16] Sebastian Madgwick. An efficient orientation filter for inertial and inertial/magnetic sensor arrays. *Report x-io and University of Bristol (UK)*, 25:113–118, 2010.

[17] Robert Mahony, Tarek Hamel, and Jean-Michel Pflimlin. Nonlinear complementary filters on the special orthogonal group. *IEEE Transactions on automatic control*, 53(5):1203–1217, 2008.

[18] Mark W Mueller, Michael Hamer, and Raffaello D'Andrea. Fusing ultra-wideband range measurements with accelerometers and rate gyroscopes for quadrocopter state estimation. In *2015 IEEE International Conference on Robotics and Automation (ICRA)*, pages 1730–1736. IEEE, 2015.

[19] Nikhil Nigam, Stefan Bieniawski, Ilan Kroo, and John Vian. Control of multiple uavs for persistent surveillance: algorithm and flight test results. *IEEE Transactions on Control Systems Technology*, 20(5):1236–1251, 2011.

[20] Alessandro Polo, Federico Viani, Enrico Giarola, Giacomo Oliveri, Paolo Rocca, and Andrea Massa. Semantic wireless localization enabling advanced services in museums. In *The 8th European Conference on Antennas and Propagation (EuCAP 2014)*, pages 443–446. IEEE, 2014.

[21] Andreas Raptopoulos, Darlene Damm, Martin Ling, and Ido Baruchin. Transportation using network of unmanned aerial vehicles, July 5 2016. US Patent 9,384,668.

[22] Antonio Ramón Jiménez Ruiz, Fernando Seco Granja, José Carlos Prieto Honorato, and Jorge I Guevara Rosas. Accurate pedestrian indoor navigation by tightly coupling foot-mounted imu and rfid measurements. *IEEE Transactions on Instrumentation and measurement*, 61(1):178–189, 2011.

[23] Davide Scaramuzza and Friedrich Fraundorfer. Visual odometry [tutorial]. *IEEE robotics & automation magazine*, 18(4):80–92, 2011.

[24] Natthapol Watthanawisuth, Adisorn Tuantranont, and Teerakiat Kerdcharoen. Design of mobile robot for real world application in path planning using zigbee localization. In *2014 14th International Conference on Control, Automation and Systems (ICCAS 2014)*, pages 1600–1603. IEEE, 2014.

[25] Yinglei Xu, Yongsheng Ou, and Tiantian Xu. Slam of robot based on the fusion of vision and lidar. In *2018 IEEE International Conference on Cyborg and Bionic Systems (CBS)*, pages 121–126. IEEE, 2018.

[26] Yuanxi Yang and Weiguang Gao. An optimal adaptive kalman filter. *Journal of Geodesy*, 80(4):177–183, 2006.

[27] Junyi Zhou and Jing Shi. Rfid localization algorithms and applications—a review. *Journal of intelligent manufacturing*, 20(6):695, 2009.